**Research Article**

# Cobalt decorated egg-shell-type activated carbon pellets: Catalytic application in hydrogen release from boron based solid fuel

**Bilge COŞKUNER FİLİZ[a]\***, **Aysel KANTÜRK FİGEN[b,c]**

*[a]Department of Metallurgy and Materials Engineering, Yıldız Technical University, Istanbul, Türkiye*
*[b]Department of Chemical Engineering, Yıldız Technical University, Istanbul, Türkiye*
*[c]Clean Energy Technologies Institute, Yıldız Technical University, Istanbul, Türkiye*

**ABSTRACT**

Hydrogen became zero-carbon fuel used in fuel-cell or internal combustion engines, regarding energy sector green-hydrogen also has become an energy carrier in commercial applications. For supporting decarbonization strategies based on hydrogen, boron-fuels are good options to safely store for mobile technologies. Ammonia borane ($NH_3BH_3$) is the one of the boron based fuels that stored 19.6 wt.% $H_2$ in its structure chemically. Cobalt (Co) decorated egg-shell-type activated carbon pellets were synthesized for catalytic application of hydrogen release from $NH_3BH_3$. Two different sized pellet type activated carbon was decorated with cobalt by combined procedure as modified vacuum-impregnation method with heat fixation and reduction. The obtained catalysts were characterized by applying optical microscope (OM), scanning electron microscope/energy dispersive X-ray spectroscopy (SEM/EDS), transmission electron microscopy (TEM), nitrogen sorption based surface analyses (BET). Activated carbon provides porous structure for effectively dispersion Co particles while the outer shell shows the catalytic activity for hydrogen generation. Structural characterization results and preliminary activity tests confirmed that fabricated Co@ACPB exhibited better performance compared with Co@ACPS catalysts thanks to thinner shell thickness and higher BET surface area/pore volume properties. The results of the kinetic study showed the core-shell type Co based catalyst catalyzed the reaction and follows the zero-order reaction kinetic model with 41.78 kJmol$^{-1}$. Activated carbon pellets provide well dispersion and stability of active Co sites, easy separation of used catalysts after the reaction and enable practical regeneration of catalytic materials.

**Cite this article as:** Coşkuner Filiz B, Kantürk Figen A. Cobalt decorated egg-shell-type activated carbon pellets: Catalytic application in hydrogen release from boron based solid fuel. Clean Energy Technol J 2023;1:1:2–11.

**\*Corresponding author.**
*\*E-mail address: bilgecoskuner@gmail.com*

## INTRODUCTION

In recent years, dynamic processes such as increasing population and developing technology have increased the demand for energy, and with the acceleration of the consumption of existing fossil fuels, the levels of greenhouse gasses in the atmosphere have increased. Our world has faced environmental problems and disasters caused by global warming. However, decreases in air pollution were detected during the global quarantine declared due to the COVID-19 health crisis. Even if these decreases have little effect on global warming, it has been seen once again that energy demands must be met from renewable and sustainable sources. The processes that started for the control of global warming in international platforms with the First World Climate Conference in 1979 continue to this day, and the European Union emphasizes the necessity of taking concrete steps for the transition to a carbon-free economy by 2050. Zeroing net greenhouse gas emissions will only be possible by using green energy technologies. These ultimate destinations might shift the energy preference into clean hydrogen [1]. The economical and environmentally friendly production and storage technologies for hydrogen based energy systems are crucial to make it commercial. Ammonia borane ($NH_3BH_3$), has several promising advantages such as nontoxicity, high stability, and high theoretical hydrogen gravimetric capacity (19.6 wt %), is an excellent chemical hydrogen gas storage medium [2]. Moreover, the high stability of its aqueous solutions is an advantage for storage, the catalytic materials are required to release hydrogen from its structure [3]. Many homogeneous and heterogeneous catalysts have been studied including precious metals, non-noble metals, oxide forms, alloys, composites and supported forms [4–6]. Between several options, Co-based catalysts showed brilliant catalytic effects [7]. The commercialization of the catalyst required some points besides being low-cost, they have to be easily recoverable.

**Highlights**

- Egg-shell type catalysts prepared by two steps procedure
- Two different sized activated carbon pellet used
- The pellet type catalyst enable easy recovery of catalyst

The rigid type of catalysts easily enable this property. Also supported catalysts lower the price by decreasing the active compound content of catalysts by homogeneously distributing the heterogeneous substance. As mentioned before, Co based catalysts meet requirements in the point of high catalytic activity, low-price and their rigid support will enhance the points [8,9].

In this work, to compare the pellet size on the catalytic activity of Co active sites on $NH_3BH_3$ dehydrogenation, egg-shell type hybrid Co-based catalysts supported on two different size extruded pellet type active carbon (small and big size) by vacuum-impregnation-reduction protocol. Their outer shell and characteristic properties were well defined by analyses such as SEM, TEM, SEM/EDS, BET. Herein, we report an active and stable egg-shell type hybrid Co-based catalyst for the dehydrogenation of ammonia borane to produce hydrogen gas.

## MATERIALS AND METHODS

### Chemicals

Ammonia borane ($NH_3BH_3$, Sigma-Aldrich, purity> 97%) was used as a hydrogen storage medium. Cobalt chloride hexahydrate ($C°Cl_2.6H_2O$, Merck, purity> 97%) and sodium borohydride ($NaBH_4$, Merck, purity>99%) were used for catalyst preparation. Two commercial active carbon pellets in different diameters (PACP) as small (SPACP) and big (BPACP) were supplied from KMC Filtre as supporting material (Table 1) and used as-received for catalyst

**Table 1.** Technical data of commercial pellets

| Pellet | Images | Raw Materials | BET Surface area, m²g⁻¹ | Mean Particle Diameter, mm |
|---|---|---|---|---|
| SPACP |  | Coal | 1000 | 2 |
| BPACP |  | Coal | 1000 | 4 |

SPACP: Small active carbon pellets; BPACP: Big active carbon pellets.

preparation. Technical data provided by the manufacturer were given in Table 1.

All chemicals used in experiments without further purification. Deionized water with 10 μs.cm⁻¹ conductivity was observed by osmosis followed by ion-exchange and filtration.

### Preparation of Egg-shell-type Catalyst

Two series of egg-shell type Co based catalysts supported on small size (Co@ACPS) and big size (Co@ACPB) extruded activated carbon pellets were prepared by two-step procedure as shown in Figure 1. Egg-shell-type pellet catalysts were prepared by selectively placing cobalt on the outer region (shell) of activated carbon pellets (egg) in three steps: (i) vacuum impregnation (at 60 °C), (ii) heat fixation (at 120 °C), (ii) in-situ reduction (at 0 °C). Typically, 3.97 g of $C°Cl_2.6H_2O$ was 50 mL of Milli-Q $H_2O$ and kept under vigorous stirring for 15 min. Then, 5 g of activated carbon pellets were added to immerse into the above aqueous $C°Cl_2$ solution and the vacuum systems was sealed and maintained at 60 °C to completely fill the pores in the activated carbon pellets. After vacuum impregnation, heat fixation was performed at 120 °C and then cooling down to room temperature naturally. The pellets were reduced with 75 ml of 0.1 M NaBH4 solution under controlled medium at 0 °C, until no bubbles were observed. Finally, the pellets were taken out, washed with distilled water to remove borate species from the external surface of the activated carbon pellet and directly used in reactions.

### Catalytic Activity Measurements

The catalytic activity of hybrid catalysts for the dehydrogenation of $NH_3BH_3$ based on hydrolysis reaction was measured by a classic water-filled gas burette system. Typically, 0.1 g of pellets were filled into a batch type jacketed round-bottom flask under vigorous stirring (200 rpm). After, 0.12 M $NH_3BH_3$ prepared by dissolving $NH_3BH_3$ in deionized water were quickly added to the flask. The volume evolved from hydrogen gas was quantified via the classical gas-burette system. The volume of produced hydrogen (ml) was measured by water displacement method. The produced hydrogen was collected up to 40 min and the produced $H_2$ gas volume was plotted against time and the production rate profiles were examined. The catalytic performance of the catalyzed hydrolysis of $NH_3BH_3$ was studied at several tem-

peratures (20 °C-80 °C), which were placed into thermostatic water bath, to get the apparent activation energy ($E_a$) of the hydrolysis of $NH_3BH_3$ catalyzed by the hybrid catalysts. The hydrogen production profiles used to calculate dehydrogenation rate (HGR) of $NH_3BH_3$. Power Law Kinetic Models (Zero, First, and Second), Arrhenius, and Eyring methods were used to examine the kinetic and thermodynamic properties of hydrogen evolution during $NH_3BH_3$ hydrolysis over pellets. The volumetric hydrogen evolution as a function of time (t, min) was translated to molar equivalent and $NH_3BH_3$ concentration ($C_{NH3BH3}$, M) and used to calculate correlation co-factors ($R_2$), kinetic and thermodynamic values. Arrhenius and Eyring plots were used to compute kinetic values such as apparent activation energy ($E_a$, kJ mol⁻¹), rate constant (k), and thermodynamic values such as activation enthalpy ($\Delta H^{\neq}$, kJ mol⁻¹) and entropy ($\Delta S^{\neq}$, J mol⁻¹) [3]. Gibbs free energy ($\Delta G^{\neq}$, kJ mol⁻¹) was also computed from the general thermodynamic equation using $\Delta H^{\neq}$ and $\Delta S^{\neq}$ values for 22 °C (Eq.3) in which Arrhenius constant ($k_0$), universal gas constant I, Boltzmann constant ($k_B$) and Planck constant (h) were used.

$$Ln(k) = \ln(k_0) + \frac{E_a}{RT} \tag{1}$$

$$\ln\left(\frac{k}{T}\right) = \ln\left(\frac{k_B}{h}\right) + \frac{\Delta S}{R} - \frac{\Delta H}{R} \cdot \frac{1}{T} \tag{2}$$

$$\Delta G^{\neq} = \Delta H^{\neq} - T.\Delta S^{\neq} \tag{3}$$

### Material Characterization

Optical microscopes (Zeiss Sycop3 axio zoom.v16) were used to determine the shell thickness of catalysts. The surface area and pore size were measured on Micrometerics Co. USA system at liquid $N_2$ temperature. Scanning electron microscopy- energy dispersive X-ray spectroscopy (SEM/EDS) measurements were performed on ZEISS EVO LS10 SEM operated at 7 kV. Samples were fixed on carbon film coated sample holders and then coated with Au-Pd. High resolution transmission electron microscopy (HR-TEM) on a Hitachi HighTech HT7700, operated at 120 kV, was used for determination of particle sizes and dispersions of Co sites on carbon pellets. In addition to this, Inductively Coupled Plasma – Mass Spectrometer (ICP-MS, Agilent 7700) techniques were used to analyze the elemental content of the spent solution (Co).
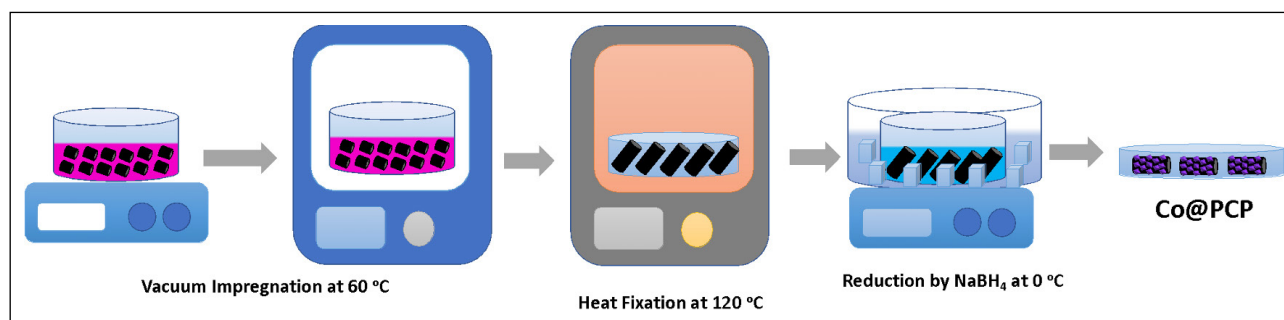


**Figure 1**. Preparation of egg-shell-type catalyst.

## RESULTS AND DISCUSSION

Benefiting from the large specific surface area of activated carbon pellets (>1000 m²g⁻¹), Co active sites could be easily loaded on the surface area of pellets with a simple method using vacuum and reduction of sodium borohydride without use of another reducing agent or stabilizers. As shown in Figure 2, the two step procedure provides an egg-shell structure Co-active carbon pellet with a uniform shell region and a core structure. Figure 2 a and d showed the shell structure of both pellets and cross-sectional photos of each catalysts obviously showed the active Co shell on the outer surface of active carbon pellets. The contact time and concentration of the C°Cl₂ solutions were the same. The thickness of the shell might not be affected only from the size of the pellets. The bigger the sample (Co@ACPB, 3.41 μm± 0.98 μm), almost the same as the impregnated shell under identical conditions compared to small one (Co@ACPS, 4.57 μm± 0.40 μm).

In line the optical micrographs recorded by optical microscope, SEM (Fig. 3) and EDS (Fig. 4) images were evidence of Co shell on the surface of active carbon pellets. Figure 3 shows the SEM images of each step of the synthesis procedure (vacuum impregnation and reduction) for both catalysts. The morphologies of samples after the Co species vacuum- impregnation procedure were quite different. At that step, Co active sites loaded on to different sized extruded active carbon pellets with the same procedure under
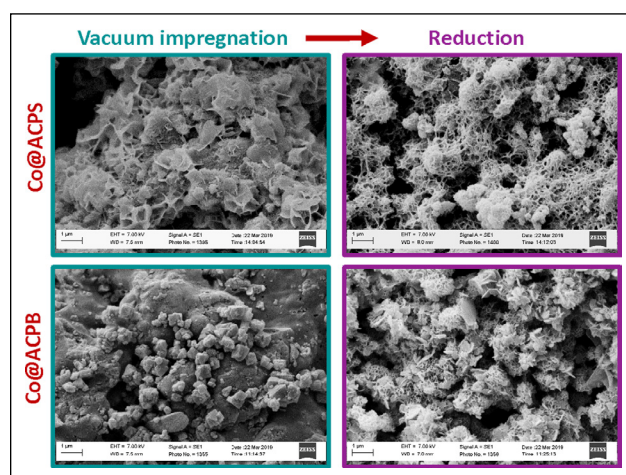


**Figure 3**. SEM images of **(a, b)** Co@ACPS and **(c, d)** Co@ACPB catalysts after vacuum impregnation and reduction, respectively at 60000 magnification.

equal conditions. Co-species covered the active carbon pellet surface, when the bigger size pellets used and more cubic shaped crystals on the surface of smaller size pellets were observed. After the reduction step, both catalysts present similar morphology that holds porous spider-net structure. These are attributed to the reduction of Co species placed on the surface of the porous pellets, resulting in a change in the morphology and structure of them.

The active component, Co, was loaded on active carbon
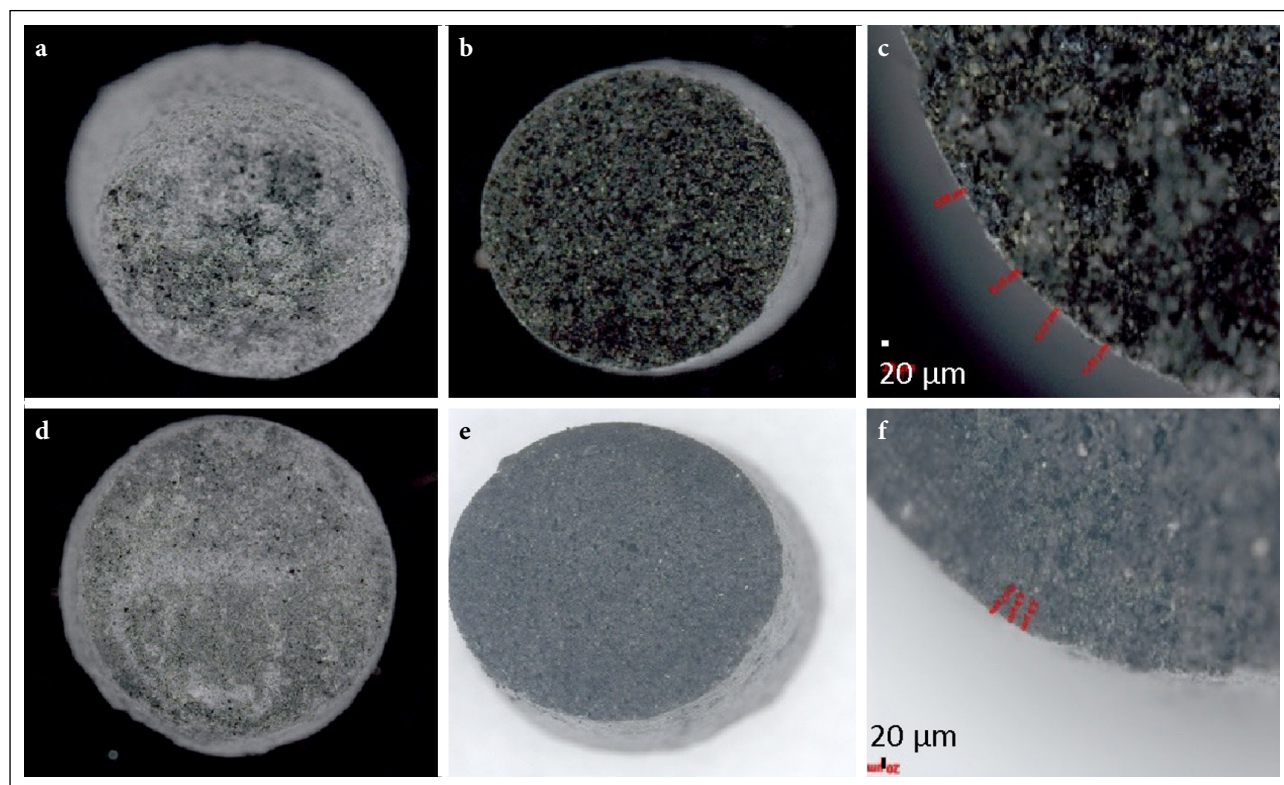


**Figure 2**. Optical micrographs of egg-shell type **(a, b, c)** Co@ACPS and **(d, e, f)** Co@ACPB catalysts.
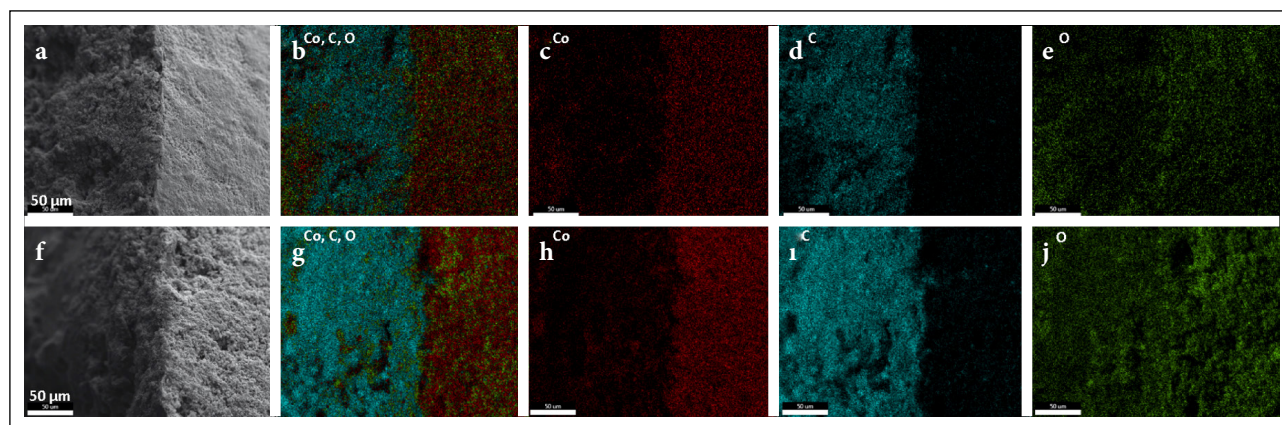
**Figure 4**. Elemental mapping results of cross-sectional area of **(a-e)** Co@ACPS and **(f-j)** Co@ACPB egg-shell type catalysts.

pellets. Noticing that Co active sites were immobilized on the active carbon surface. A two series of egg-shell like catalysts were synthesized and examined with SEM/EDS (Figs. 3 and 4). The cross-sectional photos showed that Co active sites were well dispersed and stabilized on the both active carbon pellets' surface. The etched nanoparticles had a clear egg-shell like structure with active carbon as an egg and the outer surface as the shell. The Co active species were dispersed as a one layer as a shell. The EDS images indicated that total concentration of Co active sites were the same for both pellets that indicated purple color. This confirms that of the egg-shell- type catalysts was Co concentrated only in the outer region of the pellet and desired structure was successfully obtained. The elemental content of the cross-sectional images showed that % 28 Co elemental content was observed on that area for the both samples.

The TEM analysis (see Fig. 5) of the egg-shell type catalysts were consistent with the structures indicated by SEM/EDS. The homogeneous distributions of Co shows the one layer nano-spherical particles averagely 20 nm the visually illustrated average mono-metallic clusters sizes in all catalysts were similar. The nano diameters and monodispersed size distributions of mono metallic Co particles on the pellet surface indicated that in-situ confinement on porous pellets by impregnation and reduction methods was an effective way to inhibit aggregation of the Co clusters.

Table 2 listed the morphological and structural properties of egg-shell type Co@ACPS and Co@ACPB catalysts:
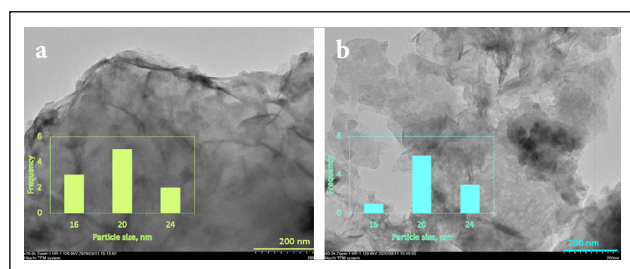


**Figure 5**. TEM images of **(a)** Co@ACPS and **(b)** Co@ACPB egg-shell type catalysts with histograms.

(i) core-shell morphology was achieved, (ii) Co@ACPB had a thinner shell thickness, (iii) similar molar content of the cobalt were observed for both catalysts, (iii) cobalt nanoparticles were formed in spherical morphology, (iv) surface was determined in mesoporous pore, (v) Co@ACPB showed higher BET surface area/pore volume ratio. In addition to this, to make a brief comparison preliminary activation tests were performed to see catalytic activity of both egg-shell type Co@ACPS and Co@ACPB catalysts over $NH_3BH_3$ dehydrogenation. Due to thicker shell thickness and large surface area/pore volume ratio Co@ACPB (0.15 mL $H_2$min$^{-1}$ g$^{-1}_{Co}$) catalyst exhibited higher catalytic activity against $NH_3BH_3$ hydrolysis compared to Co@ACPS (0.12 L $H_2$min$^{-1}$ g$^{-1}_{Co}$) at 40 °C.

The figure of merit (FOM) analysis performed for the evaluation and selection of catalytically active catalysts. In this case, five parameter used as shell thickness (S, μm), Co element (%) on surface/BET surface area (C, % Co/(m²g$^{-1}$)), Co particle size (P, nm), BET surface area/Pore volume ratio (B), hydrogen generation rate (H, ml $H_2$/min mg cat). The low and high value of parameters were defined as low (1) and high (2) levels to calculate the factor of merit and decide the efficient catalyst. The results as given In Table 3 showed that Co@ACPB was a comparatively efficient catalyst for $NH_3BH_3$ dehydrogenation with a higher factor value. For this reason, we decided to continue catalytic activity

**Table 2.** FOM Analysis results for egg-shell type catalysts

| Properties | Co@ACPS | Co@ACPB |
|---|---|---|
| S | 2 | 1 |
| C | 2 | 1 |
| P | 1 | 1 |
| B | 1 | 2 |
| H | 1 | 2 |
| Factor | 0.46 | 0.54 |

Co@ACPS: Co based catalysts supported on small size; Co@ACPB: Co based catalysts supported on big size  S: shell thickness; C: Surface area; P: Particle size; B: Volume ratio; H: Hydrogen generation rate.

**Table 3.** BET surface area, pore volume and size of freshly prepared and used catalysts in NH3BH3 dehydrogenation

| Properties | Used at 20 °C | Used at 60 °C | Used at 80 °C |
|---|---|---|---|
| BET surface area/ Pore volume ratio | 2125 | 1794 | 1747 |
| Pore size, nm | 1.87 | 2.24 | 2.29 |

BET: Based surface analyses.

and kinetic investigation tests with Co@ACPB catalysts.

The catalytic activity of the as-prepared catalyst was tested for $NH_3BH_3$ dehydrogenation. The evolved hydrogen volumes after completion of hydrogen generation from 0.12 M $NH_3BH_3$ solution on different activated carbon pellets supported Co catalysts - Co@ACPB at various temperatures (20-80 °C) were shown in Figure 6 and also Figure S1. It was clear that both catalysts were active and generated hydrogen gas instantaneously as they came in contact with the $NH_3BH_3$ solution. Hydrogen generation curves showed a typical tendency in hydrogen generation volume against time. 3 moles of hydrogen were completely released from 1 mole of $NH_3BH_3$ after 27.17 min with 0.26 L $H_2$ min$^{-1}$ g$^{-1}_{Co}$. The egg-shell type activated carbon supported Co based catalyst exhibited comparable activity with reported lit-



**Figure 6.** Hydrogen generated from $NH_3BH_3$ solution in presence of Co@ACPB at various temperature (20-80 °C): **(a)** Volume of generated and **(b)** hydrogen generation rates (HGR).

erature: 0.38 L $H_2$ min$^{-1}$ g$^{-1}_{Co3O4}$ for $Co_3O_4$ beads at 60 °C [9], 6.67 L $H_2$ min$^{-1}$ g$^{-1}$ for Cu@FeCo core–shell nanoparticles at 298 K [10], 1.44 L $H_2$ min$^{-1}$ g$^{-1}$ for amorphous Co-B nanoparticles at 25 °C [11].

In the case of Co@ACPB catalyst mixed with $NH_3BH_3$ solution, active hydrogen generation did not start immediately. The hydrogen bubbles started about 9 min after contacting with solution for 20 °C. When Co@ACPB catalyst mixed with $NH_3BH_3$ solution, the efficiency of the catalysts dramatically improved by decreasing the induction time to 4 min. Over the temperature range examined, the time required for the completion of all hydrogen gas in presence of active carbon pellet supported Co catalyst decreased with increasing temperature. The results showed that catalytic activity of the catalysts was sensitive to the temperature. The hydrolysis of $NH_3BH_3$ was incomplete with only %50 hydrogen being released in 40 min at 20 °C as shown in Figure 6 a. By increasing the temperature to 40 °C, the release of hydrogen was totally accomplished within 15 min. Further increase the temperature of the reaction to 60 °C led to a shorter reaction time (7 min) showing temperature holds a positive effect on the hydrolysis of $NH_3BH_3$. Figure 6b illustrates the hydrogen generation rates in presence of Co@ACPB catalyst with various reaction temperatures. The hydrogen generation rate performances were drastically slowed down by decreasing the temperature from 80°C to 20 °C. The HGR was decreased from 1.12 L $H_2$ min$^{-1}$ g$^{-1}$ up to 0.02 L $H_2$ min$^{-1}$ g$^{-1}$ for hydrolysis. Considering all HGR rates, the maximum hydrogen generation rate was obtained at 80°C as expected due to reaction kinetic accelerating effect.

To obtain the apparent activation energy ($E_a$) value in the dehydrogenation of $NH_3BH_3$ over Co@ACPB, the Power Law reaction kinetic models were performed for data obtained from different temperatures. As observed from Figure 7, the dehydrogenation of $NH_3BH_3$ over Co based catalysts obeyed the zero-order reaction kinetic model with their higher correlation co-factor values (>0.99) compared to first and second-order reaction kinetic models. The value of Ea for Co@ACPB was calculated to be 41.78 kJmol$^{-1}$ that was comparable with works of literature as reported: 56.53 kJ mol$^{-1}$ for Co [12], 38.19 kJ mol°C for Co ion-imprinted hydrogel [13], 45.5 kJ mol°C for Co-B [11], 33.25 kJ mol$^{-1}$ for $TiO_2$-supported RuCo catalysts [14]. Because $NH_3BH_3$ hydrolysis over Co based catalysts follows zero-order kinetics, thermodynamic parameters were also examined using Eyring's plots (Fig. S2). $\Delta H^{\neq}$ (kJmol$^{-1}$) value was 59.38 kJmol$^{-1}$, $\Delta S^{\neq}$ was -77.24 kJmol$^{-1}$K$^{-1}$ and $\Delta G_{295\neq}$ was 22.84 kJmol$^{-1}$. All obtained $\Delta H^{\neq}$ (kJ mol$^{-1}$) and $\Delta G_{\neq 295}$ (kJ mol$^{-1}$) displayed positive and $\Delta S^{\neq}$ (J K$^{-1}$ mol$^{-1}$) was negative values that demonstrating this hydrolysis reaction over pellet type catalyst was non-spontaneous, and reagents required an external energy for leveling up the reaction to transition state. And also positive value of $\Delta S^{\neq}$ indicated that this hydrolysis process over pellets was non-spontaneous, endergonic, and
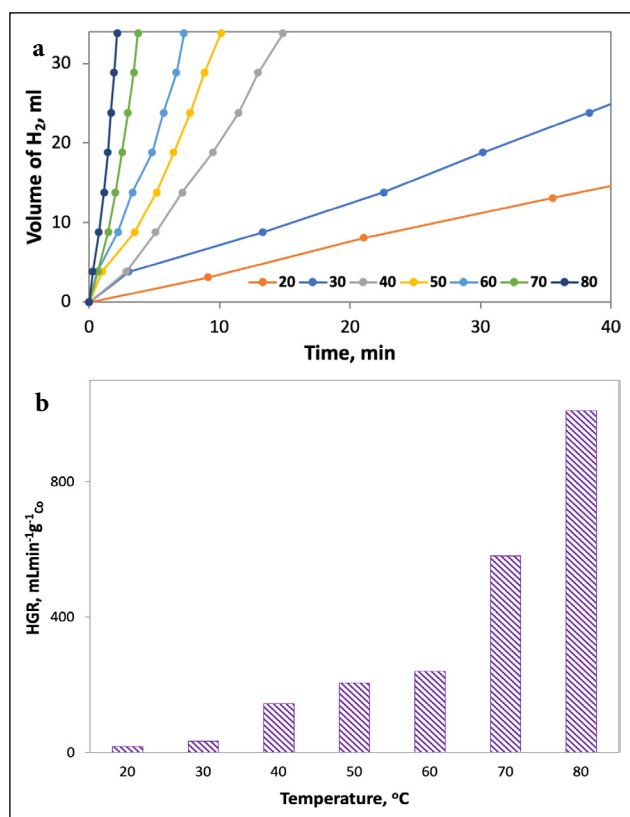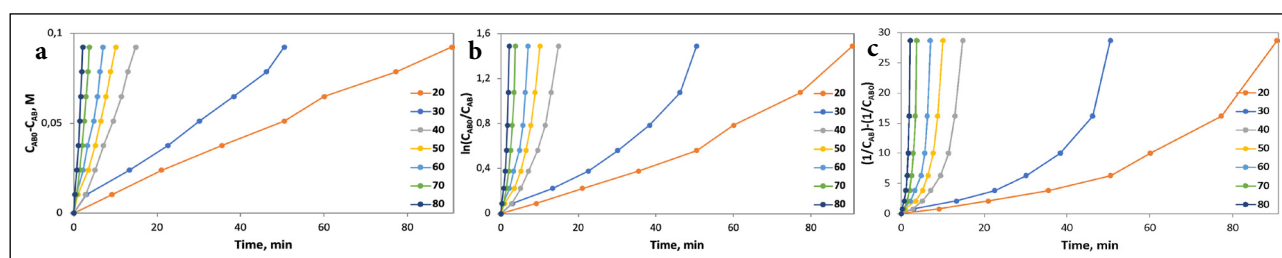
**Figure 7**. Power law kinetic models for dehydrogenation of $NH_3BH_3$ in presence of Co@ACPB: **(a)** Zero-, **(b)** First-, **(c)** Second- order models.

reagents required an external energy to level up the reaction to transition state.

The physicochemical and morphological characteristics of spent catalyst were displayed in Table 2 and 3 as well as the Co concentration results of spent $NH_3BH_3$ solutions. Table 3 showed surface area and pore changes of catalysts after dehydrogenation reactions measured by BET surface analyzer. Co@ACPB catalysts prepared from the small size of porous carbon pellets showed more stable structure and increased on their surface area was reported. The surface area of used Co@ACPB at 20 °C was decreased only about 9.68%: it decreased from 847 $m^2/g$ to 765 $m^2/g$. Together with this observation, relatively smaller surface area of the used catalysts at higher dehydrogenation compared to used samples at 20 °C were observed. The decrease of pore size of all used catalysts could be accompanied by pore blocking of by-products such as borates species [15].

The SEM images of used egg-shell type pellet catalysts were shown in Figure 8. A photographic analysis based on SEM results of spent catalysts at different temperatures (20 °C, 60 °C and 80 °C) apparently showed that residual borate species were seen at the surface area of the used catalysts, whereas not found at fresh ones. A similar structure has been reported by Chen for the $NH_3BH_3$ dehydrogenation [16]. The progressive development of borate species on the surface of pellet type catalysts was also observed. The borate species adsorbs on the metal sites causing detachment of the cobalt nanoparticles, which are located on the surface of the active carbon support. This agglomeration process probably con-

tinued until the outer layer was completely encapsulated by ammonia-borate crystals [9, 17, 18]. Even so, SEM images also confirmed that the temperature of the reaction affects the surface morphology of the used pellet catalysts.

The active Co metal leaching into spent ammonia borane solution, that had a basic property itself, was examined by the ICP-OES technique. The amount of Co in spent solution was found to be negligible as <0,0001 M Co for Co@ACPB, respectively. The results showed that this egg-shell type catalyst could be recovered and reused for several times without significant loss of Co leaching into $NH_3BH_3$ solution [19].

## CONCLUSION

In this paper, two different sized egg-shell-type porous active carbon pellet-supported cobalt nanoparticle catalysts were synthesized via vacuum impregnation-reduction procedure. The both sizes of egg-shell-type pellet catalysts had the same crystalline structure and sharply defined outer shell with totally same Co content (%). The average 20 nm Co nanoparticles were well dispersed on the surface of the porous active carbon pellets. In addition to these, the prepared bigger sized pellet type Co-catalysts has a larger surface area (847 $m^2/g$) and smaller pore size (2.27 nm). Based on the above analysis, it is obviously deduced that the size of active carbon pellet supports had an influence on the catalytic performance. Besides chemical and morphological structures showing similarity, the thickness of the active Co
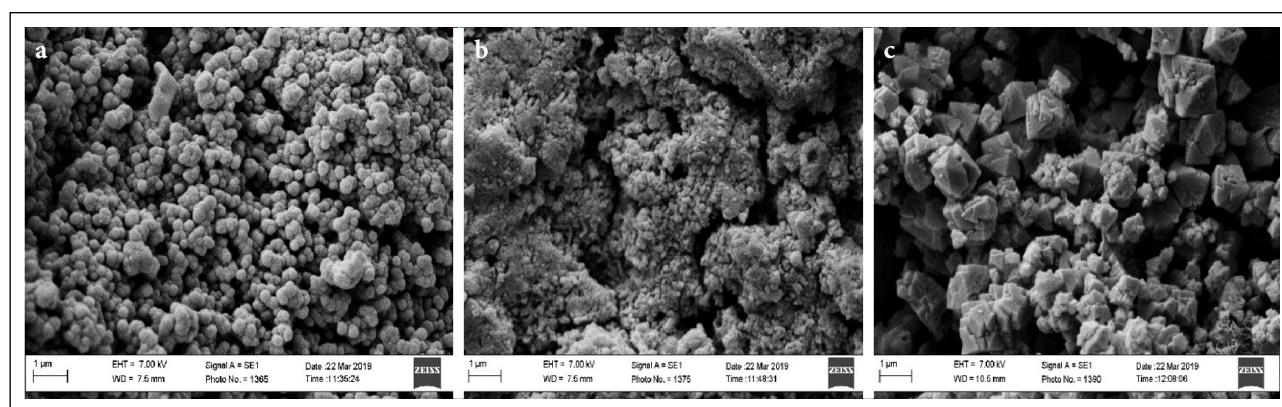


**Figure 8**. SEM images of used catalysts at 60000 magnification.

shell was changed. These results might be associated with the change in the catalytic performance and synergetic interaction between the by-products. Among two different active carbon pellets, the bigger size had presented some advantages due to it could be more easily removed after reaction completed and leaching of the Co species into spent solution was less than smaller size pellets. Also big sized pellets were more suitable for high temperature hydrolysis in which DOE criteria for hydrogen energy systems required stability at working temperature of 60 °C. Using pellet type catalysts support also made it easy to separate used catalysts after the hydrogen generation reaction completed and enable practical regeneration of catalytic materials. The egg-shell structure provides homogeneous type catalysts behavior by homogeneous dispersion of active Co sites on the surface. The egg-shell type pellet catalysts have a great potential for the in-situ hydrogen generation applications due to their easy recoverable and catalytic activity.

## ACKNOWLEDGEMENTS

## AUTHORSHIP CONTRIBUTIONS

Authors equally contributed to this work.

## DATA AVAILABILITY STATEMENT

The authors confirm that the data that supports the findings of this study are available within the article. Raw data that support the finding of this study are available from the corresponding author, upon reasonable request.

## CONFLICT OF INTEREST

The author declared no potential conflicts of interest with respect to the research, authorship, and/or publication of this article.

## ETHICS

There are no ethical issues with the publication of this manuscript.

## REFERENCES

[1] Dincer I. Covid-19 coronavirus: Closing carbon age, but opening hydrogen age. Int J Energy Res 2020;44:6093–6097. [CrossRef]

[2] Tong F, Liang X, Wang Z, Liu Y, Wang P, Cheng H, et al. Probing the mechanism of plasmon-enhanced ammonia borane methanolysis on a CuAg alloy at a single-particle level. ACS Catal 2021:10814–10823.

[3] Nugent JW, García-Melchor M, Fout AR. Cobalt-Catalyzed Ammonia Borane Dehydrogenation: Mechanistic Insight and Isolation of a Cobalt Hydride-Amidoborane Complex. Organometallics 2020;39:2917–2927. [CrossRef]

[4] Hamilton CW, Baker RT, Staubitz A, Manners I. B–N compounds for chemical hydrogenstorage. Chem Soc Rev 2009;38:279–293. [CrossRef]

[5] Sun Q, Wang N, Zhang T, Bai R, Mayoral A, Zhang P, et al. Zeolite-encaged single-atom rhodium catalysts: Highly-efficient hydrogen generation and shape-selective tandem hydrogenation of nitroarenes. Angew Chemie Int Ed 2019;58:18570–18576. [CrossRef]

[6] Yüksel Alpaydın C, Gülbay SK, Ozgur Colpan C. A review on the catalysts used for hydrogen production from ammonia borane. Int J Hydrogen Energy 2020;45:3414–3434. [CrossRef]

[7] Akdim O, Demirci UB, Miele P. A bottom-up approach to prepare cobalt-based bimetallic supported catalysts for hydrolysis of ammonia borane. Int J Hydrogen Energy 2013;38:5627–5637. [CrossRef]

[8] Geniş D, Coşkuner Filiz B, Kılıç Depren S, Kantürk Figen A. Reusable hybrid foam catalyst for hydrolytic dehydrogenation of amine adducts of borane: Porous PVA-Immobilized Co–Ru nanoparticles. Microporous Mesoporous Mater 2020;305:110363.

[9] Kinsiz BN, Coşkuner Filiz B, Kılıç Depren S, Kantürk Figen A. Nano-casting procedure for catalytic cobalt oxide bead preparation from calcium-alginate capsules: Activity in ammonia borane hydrolysis reaction. Appl Mater Today 2021;22:100952.

[10] Qiu F, Dai Y, Li L, Xu C, Huang Y, Chen C, et al. Synthesis of Cu@FeCo core–shell nanoparticles for the catalytic hydrolysis of ammonia borane. Int J Hydrogen Energy 2014;39:436–441. [CrossRef]

[11] Ma H, Ji W, Zhao J, Liang J, Chen J. Preparation, characterization and catalytic NaBH4 hydrolysis of Co-B hollow spheres. J Alloys Compd 2009;474:584–589.

[12] Sahiner N, Yasar AO, Aktas N. Dicationic poly(4-vinyl pyridinium) ionic liquid capsules as template for Co nanoparticle preparation and H2 production from hydrolysis of NaBH4. J Ind Eng Chem 2015;23:100–108. [CrossRef]

[13] Seven F, Sahiner N. Metal ion-imprinted hydrogel with magnetic properties and enhanced catalytic performances in hydrolysis of NaBH4 and NH3BH3. Int J Hydrogen Energy 2013;38:15275–15284. [CrossRef]

[14] Zhang J, Li J, Yang L, Li R, Zhang F, Dong H. Efficient hydrogen production from ammonia borane hydrolysis catalyzed by TiO2-supported RuCo cat-

alysts. Int J Hydrogen Energy 2021;46:3964–3973.

[15] Kim YS, NO HC, Choi JY, Yoon HJ. Stability and kinetics of powder-type and pellet-type iron (III) oxide catalysts for sulfuric acid decomposition in practical Iodine–Sulfur cycle. Int J Hydrogen Energy 2013;38:3537–3544. [CrossRef]

[16] Chen W, Wang Z, Duan X, Qian G, Chen D, Zhou X. Structural and kinetic insights into Pt/CNT catalysts during hydrogen generation from ammonia borane. Chem Eng Sci 2018;192:1242–1251. [CrossRef]

[17] Valero-Pedraza MJ, Alligier D, Petit E, Cot D, Gra-nier D, Adil K, et al. Diammonium tetraborate dihydrate as hydrolytic by-product of ammonia borane in aqueous alkaline conditions. Int J Hydrogen Energy 2020;5:3–11. [CrossRef]

[18] Moussa G, Moury R, Demirci UB, Miele P. Borates in hydrolysis of ammonia borane. Int J Hydrogen Energy 2013;38:7888–7895. [CrossRef]

[19] Ghorbani-Choghamarani A, Moradi P, Tahmasbi B. Ni-SMTU@boehmite: as an efficient and recyclable nanocatalyst for oxidation reactions. RSC Adv 2016;6:56458–56466. [CrossRef]

**Supporting Information**

# Egg-shell-type nano cobalt hybrid catalysts for efficient hydrogen generation from dehydrogenation of ammonia borane

**Bilge COŞKUNER FİLİZ[a]\*** ⓘ**, Aysel KANTÜRK FİGEN[b,c]** ⓘ

*[a]Department of Metallurgy and Materials Engineering, Yıldız Technical University,*
*Chemistry-Metallurgy Faculty, Istanbul, Türkiye*
*[b]Department of Chemical Engineering, Yıldız Technical University,*
*Chemistry-Metallurgy Faculty, Istanbul, Türkiye*
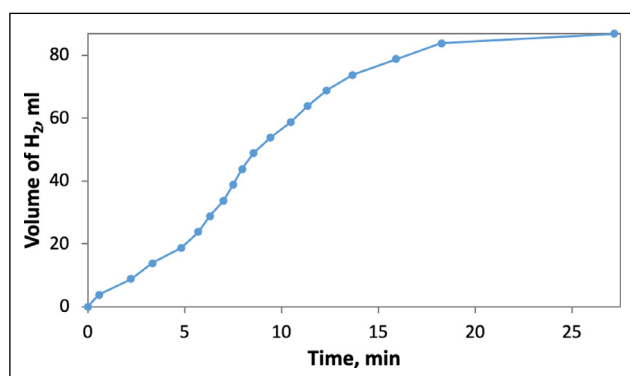
**Figure S1**. Generated hydrogen volume via $NH_3BH_3$ hydrolysis respect to time in presence of Co@ACPB catalyst at 60 °C.
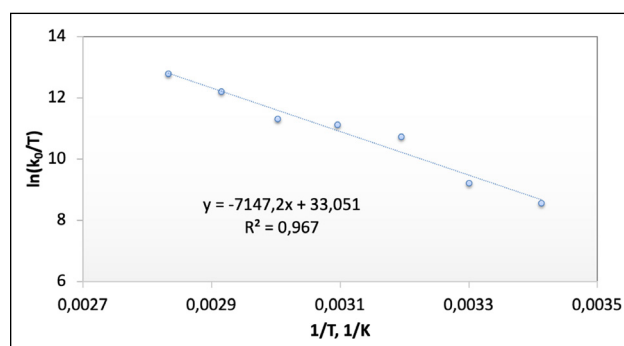


**Figure S2**. Eyring graphs of $NH_3BH_3$ hydrolysis r in presence of Co@ACPB.